

# Formulation, Configuration, and Physical Properties of Dental Composite Resin Containing a Novel $2\pi + 2\pi$ Photodimerized Crosslinker – Cinnamyl Methacrylate: An *In Vitro* Research

Murugesan Sreevarun<sup>1</sup>, Ranganathan Ajay<sup>2</sup>, Ganesan Suganya<sup>3</sup>, Vikraman Rakshagan<sup>4</sup>, Vayadadi Bhanuchander<sup>5</sup>, Karthikeyan Suma<sup>6</sup>

## ABSTRACT

**Aim:** To formulate and characterize the chemical structure of a new dental composite with photodimerized cinnamyl methacrylate (PD-CMA) photo-crosslinking comonomer and to evaluate the monomer-to-polymer conversion (MPC) and glass transition temperature ( $T_g$ ) of the new composite copolymers.

**Materials and methods:** CMA was PD by ultraviolet C-type (UVC) irradiation. The research groups were a control group C0 without PD-CMA and two trial groups: E10 (10 wt. % PD-CMA substituted in the base comonomers (B) and diluent (D) mixture); E20 (20 wt.% PD-CMA completely replacing the diluent (D) monomer). Infrared (FTIR) and nuclear magnetic resonance (NMR) spectroscopies were employed for ascertaining copolymerization (CP). The surface features and composition of the copolymers were explained by field-emission scanning electron microscopy (FESEM) and energy dispersive X-ray (EDX) spectroscopy, respectively. The MPC and  $T_g$  of the copolymers were assessed using FTIR and differential scanning calorimetry, respectively. Statistical tests were used to compare the groups.

**Results:** The configuration of the new copolymers P (BD-Co-CMA) and P(B-Co-CMA) was confirmed. The MPC% and  $T_g$  of the copolymers were better than the control. PD-CMA at 20 wt. % in the P (B-Co-CMA) copolymer exhibited the highest MPC% and  $T_g$ .

**Conclusion:** The incorporation of PD-CMA in the composite resin resulted in new P (BD-Co-CMA) and P (B-Co-CMA) copolymers with improved MPC% and  $T_g$ .

**Clinical significance:** The substitution with PD-CMA offset the shortcomings of the conventional BD comonomers concerning the mechanical properties and biocompatibility of the restorative composite resin. This might ameliorate the restorations *in vivo* longevity and serviceability.

**Keywords:** Cinnamyl methacrylate, Composite resin, Copolymerization, Cross-link, Photodimerization.

*The Journal of Contemporary Dental Practice* (2023): 10.5005/jp-journals-10024-3480

## INTRODUCTION

Commercially available dental composites mostly contain bisphenol-A-Glycerolate dimethacrylate (*Bis*-GMA) or diurethane dimethacrylate (DUDMA) as base (B) monomers along with diluent (D) monomer, commonly, triethylene glycol dimethacrylate (TEGDMA).<sup>1,2</sup> The combination of these comonomers can be designated as BD. These comonomers copolymerize with each other without any hindrance at various ratios.<sup>3</sup> Owing to the high viscosity of *Bis*-GMA, it's impractical to incorporate fillers in the matrix which ultimately led to low monomer-to-polymer conversion (MPC). Nevertheless, the quantity of the diluent TEGDMA is critical since the greater the concentration, the greater the polymerization shrinkage.<sup>4</sup>

Deficiency in the MPC and microgel agglomeration are the unsolved problems with the dimethacrylates polymerized through free radicals. Stereotyped dental composites attain 50–75% MPC, approximately.<sup>5–7</sup> *Bis*-GMA homopolymer networks possess restricted MPC as low as 50%<sup>8–11</sup> due to sol fraction existence which renders it impractical for clinical applications.<sup>5,12</sup> Lately, thermal analytical techniques have been employed to quantitatively deduce the variegated structure of polymeric networks. Heat capacity variations during glass transition and polymerizing enthalpy are determined by differential scanning calorimetry (DSC).<sup>13</sup> The polymeric chain movements are restricted below the glass transition temperature ( $T_g$ ) and above this temperature leads to chain deterioration.<sup>14</sup>

<sup>1</sup>Department of Dentistry, Vinayaka Missions Medical College & Hospital (VMRF-DU), Karaikal, Puducherry, India

<sup>2</sup>Department of Prosthodontics and Crown and Bridge, Vivekanandha Dental College for Women, Namakkal, Tamil Nadu, India

<sup>3</sup>Department of Pharmacology, Vinayaka Missions Medical College & Hospital (VMRF-DU), Karaikal, Puducherry, India

<sup>4</sup>Department of Prosthodontics and Implant Dentistry, Saveetha Dental College and Hospital, Saveetha Institute of Medical and Technical Sciences, Chennai, Tamil Nadu, India.

<sup>5</sup>Department of Prosthodontics and Crown and Bridge, Army College of Dental Sciences, Secunderabad, Telangana, India

<sup>6</sup>Department of Prosthodontics and Crown and Bridge, Government Dental College, Cuddalore, Tamil Nadu, India

**Corresponding Author:** Ranganathan Ajay, Department of Prosthodontics and Crown and Bridge, Vivekanandha Dental College for Women, Namakkal, Tamil Nadu, India, Phone: +91 8754120490, e-mail: jrjangclassiq@gmail.com

**How to cite this article:** Sreevarun M, Ajay R, Suganya G, *et al.* Formulation, Configuration, and Physical Properties of Dental Composite Resin Containing a Novel  $2\pi + 2\pi$  Photodimerized Crosslinker – Cinnamyl Methacrylate: An *In Vitro* Research. *J Contemp Dent Pract* 2023;24(6):364–371.

**Source of support:** Nil

**Conflict of interest:** None

The  $T_g$  also indirectly measures the extent of cross-linking in a copolymer. Immensely cross-linked copolymers are highly immune to deterioration and solvent sorption due to inadequate space for solvent slithering and diffusion within the resin matrix network.<sup>15</sup> Therefore, a copolymer with a linear polymeric chain is highly susceptible to solvent softening or thermal assaults when compared to a cross-linked copolymeric network.<sup>15,16</sup> Hence, MPC% and  $T_g$  are considered to be the pivotal criteria in dictating the clinical performance of dental composite resins.

To revamp the dental acrylic resins, a multitude of customizations in the base propriety monomers were studied.<sup>17-20</sup> Despite these alterations in the composite resin matrix monomers, compromised MPC, curing shrinkage, and matrix deterioration are some unsolved problems yet. Myriad novel monomers have been invented to overcome these lacunae. A dental composite resin should be biocompatible and controllable with extraordinary surface and physical properties. To suffice these requirements, this research focused exclusively on photoreactive groups or cinnamic acid ester photocrosslinkers, cinnamyl methacrylate (CMA). Cinnamic acid ester monomers photodimerized (PD) by ultraviolet (UV) irradiation leads to the formation of cyclobutane-ringed core structure which is employed in the production of photocrosslinked polymers.<sup>21-23</sup> Structurally, cinnamyl compounds contain an aromatic ring at the  $\beta$ -position of an  $\alpha$ ,  $\beta$ -unsaturated carbonyl group. Conspicuously, polymerization at the C=C moiety would yield biopolymers with a linear saturated structural rigid backbone with alternative aromatic rings and ester moieties as side chains. Such polymers are potential multifunctional biopolymers that combine polystyrene and acrylic resin features with high heat resistance owing to the aromatic side chains and the ditacticity interaction.<sup>24</sup>

There are no studies concerning the CMA incorporation in dental composite resins as a photo-crosslinker. Nonetheless, determining the interaction and copolymerization (CP) of the CMA with the BD monomers portrays an acute central role since CP determines the resin's properties. Hence, the current research aimed to formulate a novel dental composite composition with PD-CMA comonomer, characterize the chemical structure of the resultant novel copolymer and evaluate the physical properties of the composite copolymer. The null hypothesis was that the incorporation of PD-CMA in the composite resin would not

undergo CP with the BD comonomers and would not influence the MPC and  $T_g$ .

## MATERIALS AND METHODS

### Photodimerization of CMA

The CMA was pipetted in a clear glass dappen dish and exposed to UV-C light (275 nm; Mateminco MT07 UVC torch) at a distance of 20 mm in a dark room for 30 minutes. The PD was ascertained by Fourier transform infrared (FTIR) (Bruker-Tensor 27 model, Germany) and nuclear magnetic resonance ( $^1\text{H-NMR}$ ; Fig. 1B) (Bruker-Ascend™ 500, Germany) spectroscopies. Four differences (D1–D4) were observed in the IR spectra of the CMA monomer and PD-CMA (Fig. 1A). The FTIR peaks ( $\text{cm}^{-1}$ ) at 1496.73 attributed to  $^{\delta}\text{C-C}$  cyclo-dimer (D1), 1375.26, 1317.62 attributed to  $^{\delta}\text{C-H}$  cyclobutane ring (D2), and 963.24, 938.80, 792.63, 765.86, 743.63 attributing C-H cyclobutane ring breathing (D3 and D4) evince the PD of CMA. These peculiar peaks were absent in the monomer's spectrum. In  $^1\text{H-NMR}$  (400 MHz;  $\text{CDCl}_3$ ;  $\delta$ ) spectroscopy, chemical shift peaks at 3.551 (protons in cyclobutane ring distal to the phenyl ring) and 4.802 (protons in cyclobutane ring proximal to the phenyl ring) indicate the PD of CMA. These exclusive proton peaks were absent in the CMA monomer's spectrum.

### Specimens and Groups

The materials employed in the study were tabulated in Table 1. Formulation of the resin matrices and specimen preparatory as well as photo-polymerization steps for both control and trial groups strictly adhered to the method described by Sivakumar et al.<sup>18</sup> The composition of composite matrices of control (C0) and trial groups (E10 and E20) and their corresponding resultant copolymers were presented in Table 2. The total matrix:filler ratio 30:70 wt. % was maintained constant in all the groups. PD-CMA substituted 10 wt.% of TEGDMA in E10 and completely replaced TEGDMA in E20.

### FTIR Spectroscopy and Monomer-polymer Conversion

The CP and MPC of the photo-polymerized specimens (CP:  $n = 1$ ; MPC%:  $n = 10$ ) were established by the FTIR-attenuated total reflection (FTIR-ATR) spectroscopy. Initially, the spectra of non-polymerized specimens and eventually, photo-polymerized specimens were obtained. The absorption peaks representing

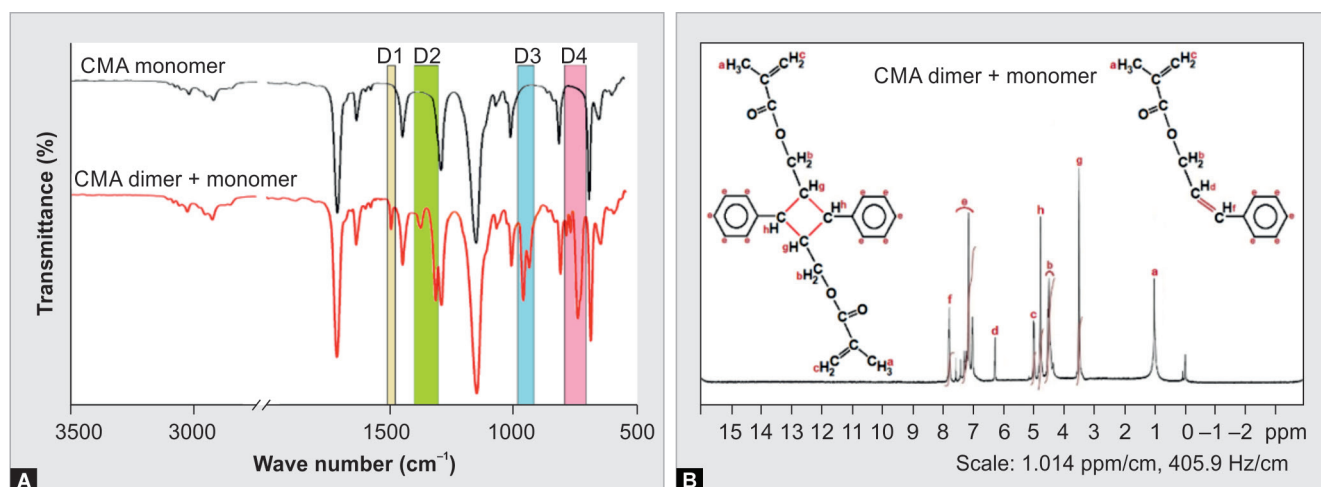


Fig 1A and B: Photodimerization of CMA; (A) IR spectra; (B)  $^1\text{H-NMR}$  spectrum

aliphatic C = C and aromatic C = C stretches were considered and appropriate baselines were drawn dividing the two peaks into two Lorentzian curves. The absorption intensities were resolved by calculating the peaks' area.<sup>25</sup> MPC% was computed employing the hereunder equation:

$$\text{MPC\%} = \left[ 1 - \frac{\left( \frac{\text{Aliphatic C = C}}{\text{Aromatic C = C}} \right)_{\text{polymerized}}}{\left( \frac{\text{Aliphatic C = C}}{\text{Aromatic C = C}} \right)_{\text{Non-polymerized}}} \right] \times 100.$$

### NMR and FESEM-EDX Spectroscopies

<sup>1</sup>H- and <sup>13</sup>C-NMR spectra of the specimens ( $n = 1/\text{group}$ ) were acquired by the NMR spectrometer with tetramethylsilane serving as the internal standard. For <sup>1</sup>H- and <sup>13</sup>C-NMR, fine ground powder (<sup>1</sup>H-NMR: 5 mg; <sup>13</sup>C-NMR: 100 mg) of the polymerized specimens was dissolved in deuterated chloroform (CDCl<sub>3</sub>) in a thin glass tube. On photo-polymerized archetypal cuboidal specimens ( $n = 1/\text{group}$ ), the topography of fractured unfinished surface was examined using field emission scanning electron microscopy (FESEM; Carl Zeiss, Supra 55VP, Germany). The mass percentage of each constituent in the specimen was detected by energy dispersive X-ray (EDX) spectroscopy (JEOL-JSM-IT 200; Tokyo, Japan).

### Glass Transition Temperature

For each group, ten polymerized specimens ( $n = 10/\text{group}$ ) were powdered, and 20 mg powder was heated on an alumina crucible

to temperatures ranging from 30–185°C at 20°C min<sup>-1</sup> rate in a differential scanning calorimetry (DSC) instrument (Netzsch, STA 449 F3 Jupiter®, Selb, Germany) under nitrogen. The  $T_g$  was deduced by following the method briefed by Ajay et al.<sup>26</sup>

### Statistical Analysis

The data analysis was worked with statistical package for the Social Sciences Software (SPSS Inc., Chicago, IL, USA; version 21.0). Concerning MPC and  $T_g$ , the data were distributed normally (Kolmogorov-Smirnov test:  $p > 0.05$ ) and thus were presented as mean and standard deviation (SD). One-way ANOVA and *post hoc* Tukey multiple comparison tests ( $\alpha = 0.05$ ) were employed to analyze differences among and between the groups, respectively.

## RESULTS

### Copolymerization

The CMA monomer successfully copolymerized with the BD comonomers resulting in P (BD-Co-CMA) copolymer of E0 group and P (B-Co-CMA) copolymer of E20 group. Table 3 tabulates the functional group attributions of the resultant copolymers by FTIR spectroscopy. In the FTIR spectra, there were nine distinctions (D) between the control and trial groups (Fig. 2). The peaks at D1, D4, D5, D6, and D8 in both the trial groups corresponding to the olefinic moiety of CMA are absent in the C0 group. This serves as evidence for CMA incorporation in the base matrix. The peak at D2 in C0 corresponds to the presence of unsaturated aliphatic C = C bonds indicating the presence of unreacted CMA or BD comonomers. Surprisingly, this peak was absent in the E10 and E20 groups, indicating no or less unreacted comonomers. The peaks at D3, D7, and D9 evince the cyclobutane ringed structure and confirm the presence of PD-CMA in the copolymers of E10 and E20.

<sup>1</sup>H-NMR (CDCl<sub>3</sub>;  $\delta$ ): 6.4 and 7.8 (–CH=CH–);  $\delta$  7.0 – 7.5 [ring protons (○H)] indicate the addition of CMA in the resin matrix; 3.7 and 4.7 [–CH≡□CH–; doublet of doublets (dd)] indicate the presence of cyclo-dimerized CMA in the matrix (Figs 3A to C). <sup>13</sup>C-NMR (CDCl<sub>3</sub>;  $\delta$ ): 117.20, 118.32, and 146.90 (–CH=CH–); 134.30 [ipso carbon (○C)] indicate the presence of CMA in the matrix; 43.2, 43.3, 51.2, and 53.1 (–CH≡□CH–) evince cyclo-dimerized CMA in the matrix (Figs 3D to F). Proton in –CH<sub>2</sub>–C– aliphatic copolymeric backbone chain (<sup>1</sup>H-NMR  $\delta$ : 2.01 – 2.23) and linking carbon in –CH<sub>2</sub>– (<sup>13</sup>C-NMR  $\delta$ : 22.17 – 23.30) conspicuously evince CP of the comonomers and CMA. The absence of proton and carbon corresponding to unsaturated double bond =CH<sub>2</sub> in the trial groups (E10 and E20) shall be inferred as no or less unreacted comonomers. The absence of proton peaks attributing –CH<sub>2</sub>–O–/–O–CH<sub>2</sub>– at  $\delta$ 3.595 – 3.687 and –CH<sub>2</sub>–methacrylate moiety at  $\delta$ 3.934 – 3.965 and

**Table 1:** Materials used in the research

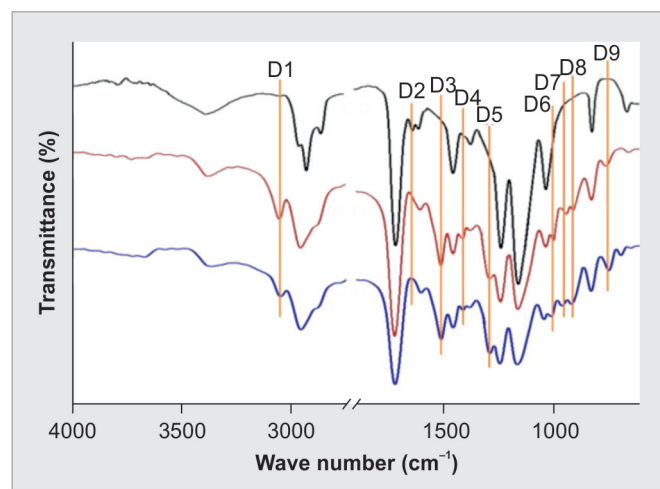
Material	Manufacturer
CMA	Polysciences, Inc., Warrington, PA, USA.
Bis-GMA	Sigma Aldrich Co., St Louis, MO, USA.
TEGDMA	
DUDMA	
Photoinitiator: Camphorquinone (CQ)	
Amine: Dimethyl aminoethyl methacrylate (DMAEMA)	
Barium oxide	
Yttrium-stabilized zirconia (YSZ) nanoparticles	
Barium fluoride	Sisco research laboratories Pvt. Ltd. Maharashtra, India.

**Table 2:** Composition of control and trial matrices and resultant copolymer

Matrix	Composition and copolymer
C0	Base comonomers: Bis-GMA (50 wt. %) + DUDMA (30 wt. %) - B. Diluent: TEGDMA (20 wt. %; D). Filler ingredients: BaO (30 wt. %), BaF <sub>2</sub> (30 wt. %), YSZ (40 wt. %). The total CQ:DMAEMA (1:2) is 1 wt. %. <b>Copolymer: P (BD)</b>
E10	Base comonomers: Bis-GMA (50 wt. %) + DUDMA (30 wt. %) - B. PD-CMA (10 wt. %) photo-crosslinker. Diluent: TEGDMA (10 wt. %; D). Filler ingredients: BaO (30 wt. %), BaF <sub>2</sub> (30 wt. %), YSZ (40 wt. %). The total CQ:DMAEMA (1:2) is 1 wt. %. <b>Copolymer: P (BD-Co-CMA)</b>
E20	Base comonomers: Bis-GMA (50 wt. %) + DUDMA (30 wt. %) - B. PD-CMA (20 wt. %) photo-crosslinker. Diluent: Absent. Filler ingredients: BaO (30 wt. %), BaF <sub>2</sub> (30 wt. %), YSZ (40 wt. %). The total CQ:DMAEMA (1:2) is 1 wt. %. <b>Copolymer: P (B-Co-CMA)</b>

**Table 3:** FTIR characteristics of the composite copolymers

Functional group characteristics of the copolymers	Group [Wave numbers (cm <sup>-1</sup> )]		
	C0 P (BD)	E10 P (BD-Co-CMA)	E20 P (B-Co-CMA)
O-H stretching	3380.28	3379.13	3364.32
C-H stretching; symmetric vibration of <i>cis</i> -HC=CH-	<b>Absent</b>	<b>3058.77</b>	<b>3052.99</b>
N-H and aliphatic chain -CH <sub>2</sub> - (C-H) stretching	2921.95	2957.07	2957.90
C = O stretching	1710.42	1723.00	1728.90
C = C aliphatic stretching (methacrylate)	<b>1634.18</b>	<b>Absent</b>	<b>Absent</b>
C = C aromatic stretching ( <i>Bis</i> -GMA/CMA)	1608.07	1608.04	1605.03
<sup>δ</sup> C - C stretching of cyclodimer	<b>Absent</b>	<b>1514.02</b>	<b>1513.36</b>
C - H bending (-CH <sub>3</sub> )	1453.98	1460.01	1459.10
<sup>δ</sup> C - H rocking vibration olefinic -HC = CH-	<b>Absent</b>	<b>1415.60</b>	<b>1417.52</b>
C - H bending (CHO; aldehyde)	1376.15	1383.70	1384.54
<sup>δ</sup> C - H bending; olefinic -HC = CH-	<b>Absent</b>	<b>1296.02</b>	<b>1296.02</b>
C-N amine stretching	1240.90	1247.15	1246.26
C-O stretching of aliphatic ester (-C(O) -O-CH <sub>2</sub> -)	1163.81	1168.66	1167.46
C-OH stretching (equatorial) of secondary alcohol	1040.88	1043.91	1044.77
<i>trans</i> -C = C out-of-plane bending, di-substituted alkene (-HC = CH-)	<b>Absent</b>	<b>1006.73</b>	<b>1014.44</b>
Aliphatic ring breathing (cyclobutane)	<b>Absent</b>	<b>950.54</b>	<b>962.63</b>
<i>cis</i> -C = C bending, di-substituted alkene (-HC = CH-)	<b>Absent</b>	<b>919.94</b>	<b>916.09</b>
N-H out-of-plane deformation of secondary aliphatic amine	824.04	830.48	830.24
Aliphatic ring vibration (cyclobutane)	<b>Absent</b>	<b>762.90</b>	<b>749.44</b>
Aromatic ring C-H wagging ( <i>Bis</i> -GMA/CMA)	648.09	654.40	694.11

**Fig. 2:** IR spectra of the groups showing nine spectral differences

the absence of carbon peaks attributing -CH<sub>2</sub>-CH<sub>2</sub>-O- moiety at  $\delta$ 77.01 - 77.33 in P (B-Co-CMA copolymer (E20 group) clearly shows the absence of TEGDMA.

**Note:** Kindly note the square and hexagon shape denote the cyclobutane carbons and phenyl ring carbons respectively.

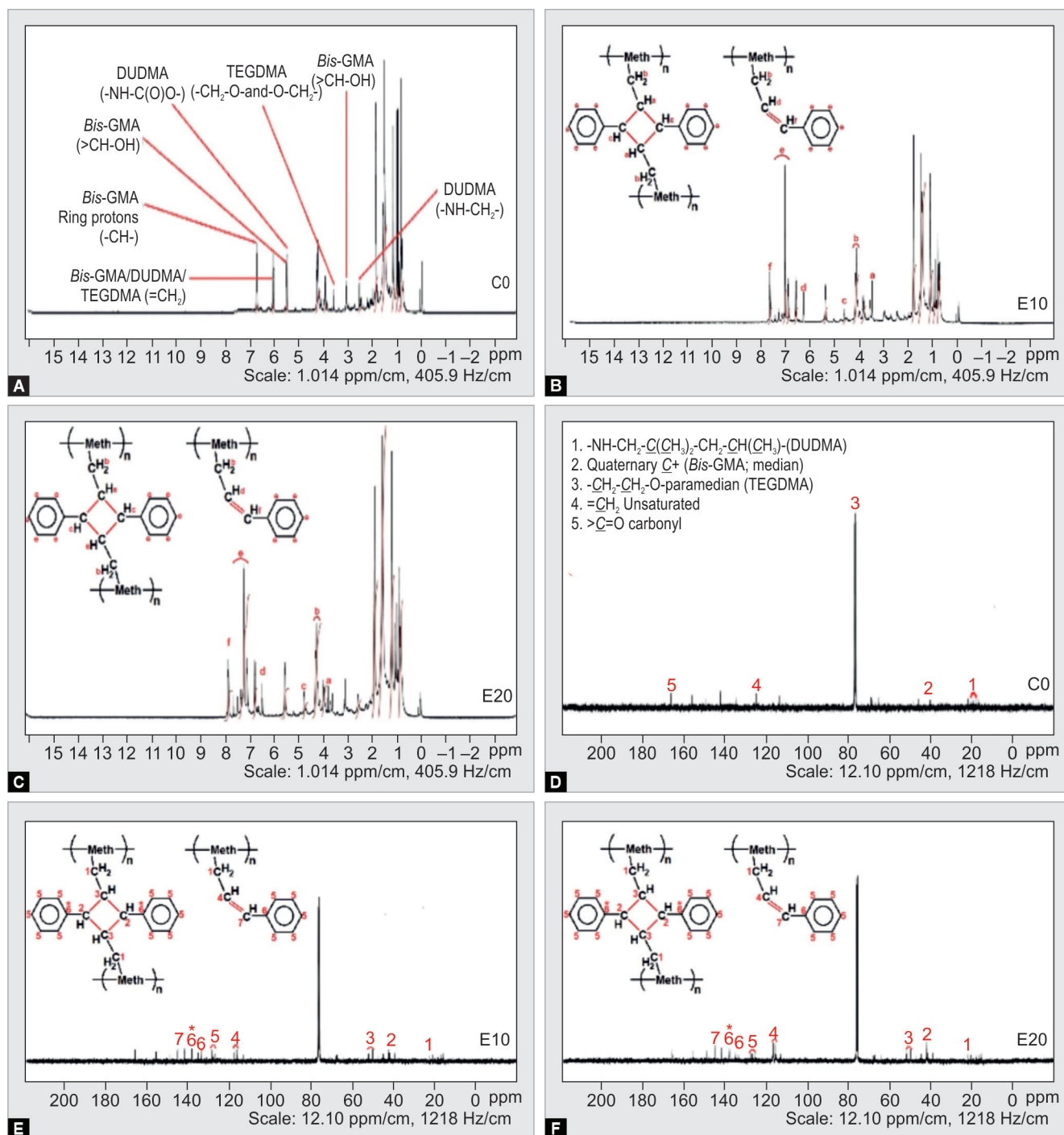
EDX spectroscopies of all the groups showed the presence of C, O, Zr, Ba, and F atoms. In the FESEM of C0, the unfinished surface appeared

rough and irregular (Fig. 4A). On the contrary, the surface of E10 and E20 appeared smooth and regular of which E20 possessed the smoothest surface free of observable defects (Figs 4B and C). This indicates that the PD-CMA formed active crosslink networks with no confined domains by eschewing cyclization by TEGDMA. Hence, the addition of PD-CMA improved the surface quality of the P (BD-Co-CMA) and P (B-Co-CMA) composite copolymers by crosslinking the matrix comonomers.

### Monomer-polymer Conversion and Glass Transition Temperature

The mean ( $\pm$  standard deviation (SD)) MPC% of C0, E10, and E20 were 67.58%, 76.21%, and 85.05%, respectively (Table 4). There was a significant difference among the groups ( $p = 0.000$ ). The MPC% of the control group was lesser than the trial group. Between the trial groups, E20 possessed higher conversion than E10. The mean  $T_g$  of C0, E10, and E20 were 90.73°C, 110.01°C, and 112.94°C, respectively, and exhibited a statistically significant difference among the groups ( $p = 0.000$ ) (Table 4). Table 5 represents the multiple comparisons between the groups. All the comparisons exhibited statistically significant differences ( $p = 0.000$ ) for both MPC% and  $T_g$ . Figure 5 depicts the IR graphs delineating the distinction in the peak intensities between the cured and uncured specimens. Figure 6 portrays the thermogravimetric curves of all the groups. Therefore, the addition of PD-CMA in the resin matrix increased the MPC% and  $T_g$  of the trial composite copolymers P (BD-Co-CMA) and P (B-Co-CMA).





Figs 3A to F: (A to C)  $^1\text{H-NMR}$  spectra of the groups; (D to F)  $^{13}\text{C-NMR}$  spectra of the groups

## DISCUSSION

Dimethacrylates CP ensues a cross-linked copolymer whose physicomechanical properties rely on the MPC% and resultant network configuration.<sup>27</sup> The hydroxyl (-OH) groups (strong hydrogen bonding) and the central aromatic ring  $\pi$ - $\pi$  interactions in the *bis*-GMA homopolymer elicit low MPC%.<sup>9,28</sup> Therefore, *bis*-GMA is usually substituted with low-viscosity monomers like TEGDMA which increases water sorption, decreases general mechanical properties, and hinders color stability.<sup>29-31</sup> Nevertheless, amongst

the dimethacrylates, TEGDMA is highly susceptible to cyclization or cyclopolymerization at the functional terminals during polymerization owing to its low viscosity and high mobility during polymerization.<sup>32</sup> This results in high conversion and less cross-linking that deteriorates the physicomechanical properties of the composite by the plasticizing effect of unreacted/unpolymerized C = C moiety.<sup>32,34</sup> Hence, in the present research, CMA was selected to substitute and replace TEGDMA. This is because dimerized CMA is hydrophobic without the hydrophilic ethoxy (-CH<sub>2</sub>-CH<sub>2</sub>-O-) moiety in contrast to TEGDMA.

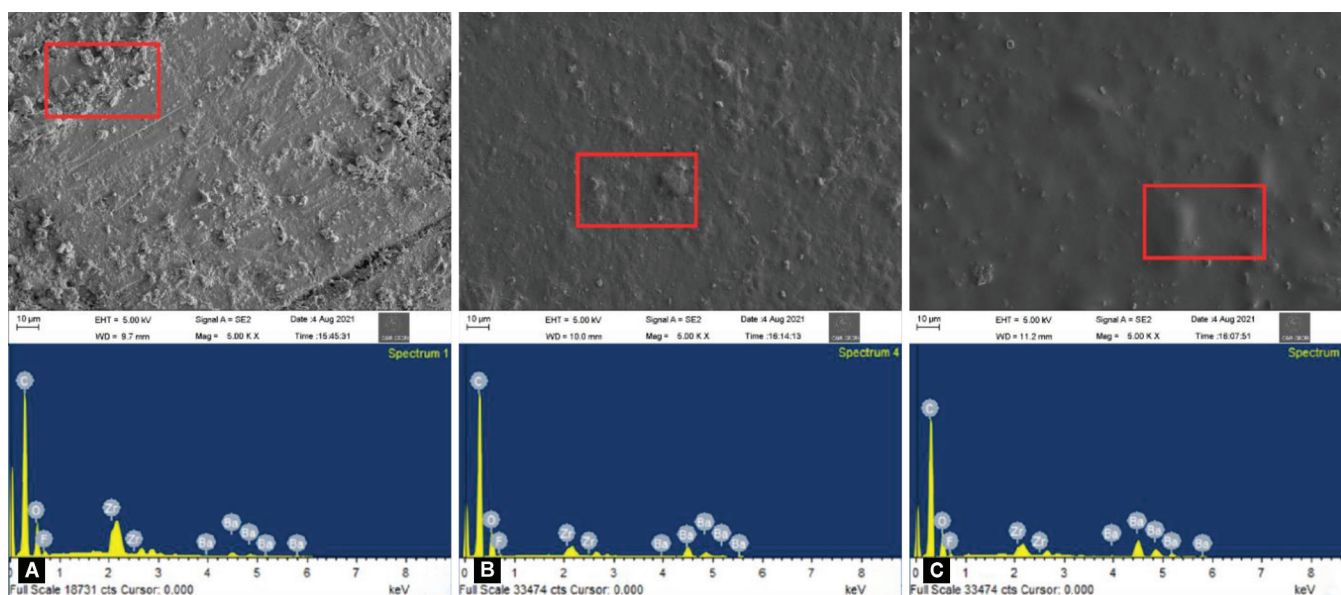


Fig 4A to C: FESEM and EDX spectra of (A) C0; (B): E10; (C): E20

Table 4: One-way ANOVA – Comparison among the groups

Group	Mean $\pm$ SD ( $^{\circ}$ C)	f-value	p-value
MPC (%)			
C0	67.58 $\pm$ 0.96	692.54152	0.000
E10	76.21 $\pm$ 1.14		
E20	85.05 $\pm$ 1.03		
$T_g$ ( $^{\circ}$ C)			
C0	90.73 $\pm$ 0.58	2619.83514	0.000
E10	110.01 $\pm$ 1.05		
E20	112.94 $\pm$ 0.45		

Table 5: Post hoc Tukey HSD multiple comparison test

Group (i)	Compared group (j)	Mean difference (i - j)	Q-value	p-value
MPC (%)				
C0	E10	-8.63*	-25.99	0.000
	E20	-17.47*	-52.63	0.000
E10	E20	-8.84*	-26.64	0.000
$T_g$ ( $^{\circ}$ C)				
C0	E10	-19.28*	-81.78	0.000
	E20	-22.21*	-94.22	0.000
E10	E20	-2.93*	-12.44	0.000

\*Mean difference is significant at 0.05 level

In this present research, the photodimerization of CMA was confirmed through IR and  $^1\text{H-NMR}$  spectroscopies. The photodimerization was a pivotal step in this research because difunctionality, or in simpler terms, at least two polymerizable groups are mandatory for a monomer to act as a cross-linker. CMA has one polymerizable  $\text{C}=\text{C}$  group; hence, it was PD to have two  $\text{C}=\text{C}$  polymerizable groups (PD-CMA). Usually, the dimers of

cinnamic acid and its derivatives including CMA exist in  $\alpha$ - and  $\beta$ - types. The  $\alpha$ -type forms by topotactic reactions where the dimerization is head-to-tail and the  $\beta$ -type forms head-to-head dimerization.<sup>35</sup> The variations between these two forms can be differentiated with Raman-phonon IR or FT-IR spectroscopies. However, in the present research, identifying the form of the PD-CMA is beyond the scope of discussion.

In the current research, the MPC% and  $T_g$  of the new copolymer P (BD-Co-CMA) were evinced by the substitution with the dimerized CMA photo-crosslinking comonomer. To forge the novel P (BD-Co-CMA) copolymer, the composition of the BD composite resin was chemically altered by the partial or complete substitution of TEGDMA by dimerized CMA (10 and 20 wt.%). In the trial groups, the FTIR peaks attributable to the presence of olefinic moiety and cyclobutane ringed-structure (D1 and D3-D9), additional protons attributable to ( $-\text{CH}=\text{CH}-$ ), ( $-\text{CH}\square\text{CH}-$ ), and additional C-atoms attributable to ( $-\text{CH}=\text{CH}-$ ), ( $\square\text{C}$ ), ( $-\text{CH}\square\text{CH}-$ ) in the NMR spectroscopies confirmed the presence of CMA in either monomer or dimer form. The formation of the new copolymer P (BD-Co-CMA) was declared by the presence of protons in the aliphatic copolymeric backbone chain ( $-\text{C}-\text{CH}_2-\text{C}-$ ) and the linking carbon ( $-\text{CH}_2-$ ) in the copolymeric structure. Likewise, the new DUDMA monomer with two quaternary ammonium groups and chlorinated *bis*-GMA were tailored and validated the structure through FTIR-ATR and NMR spectroscopies.<sup>36,37</sup> Therefore, in the current research, IR, NMR, and EDX spectroscopies were used to configure the P (BD-Co-CMA) and P (B-Co-CMA) copolymers.

The MPC% of the trial groups was greater than in the C0 group. This may be attributed to the structure of PD-CMA which has two peripheral aromatic rings without  $-\text{OH}$  group in contrast to *bis*-GMA and could have circumvented the cyclization in contrast to TEGDMA. The Abs peak at  $1637\text{ cm}^{-1}$  in the IR spectra of the C0 group signifies the presence of an unpolymerized functional group ( $\text{C}=\text{C}$ ) or residual monomer. The absence of this Abs peak for the P (BD-Co-CMA) and P (B-Co-CMA) copolymers in this research indicates that it has a higher DC and less residual monomer than the G0. In the FTIR and NMR spectra of the trial groups E10 and E20, both olefinic moiety and cyclobutane ring moiety were present. This is attributed

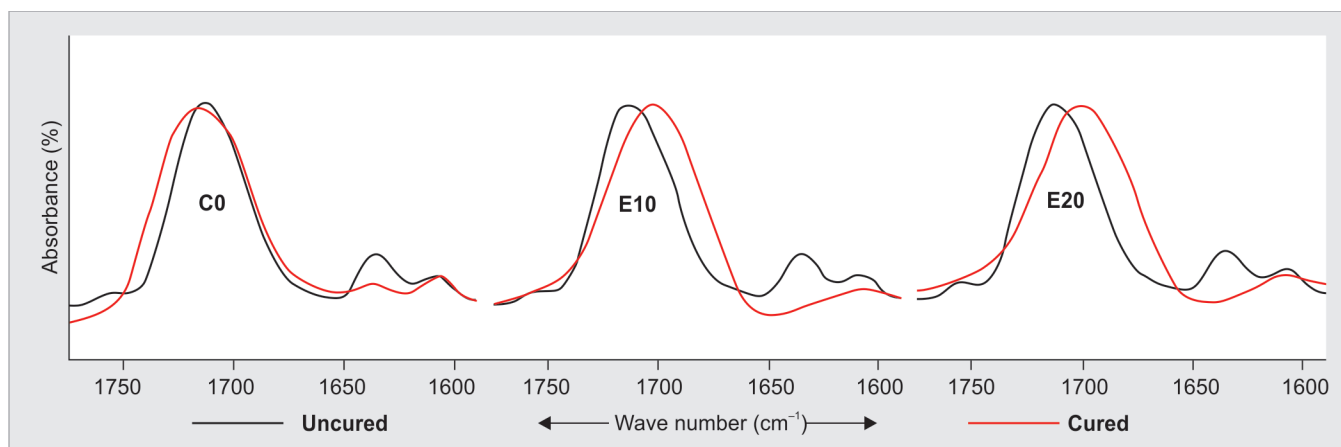


Fig. 5: IR spectra depicting the MPC of the groups

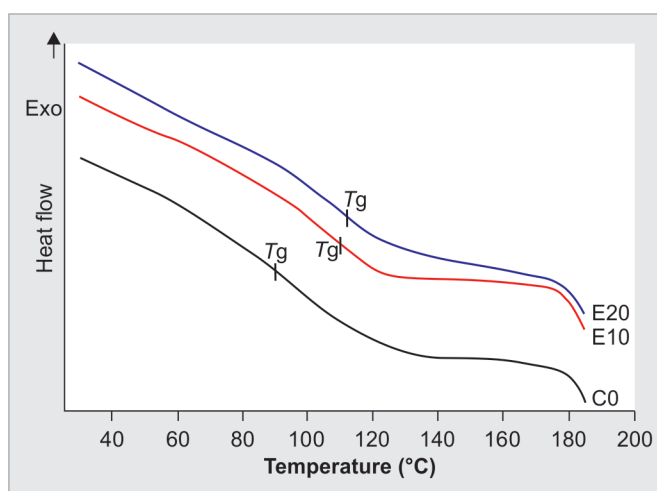


Fig. 6: Thermogravimetric curves of the groups with  $T_g$  plot

to the photodimerization time when the CMA was PD for 30 min. Panda and Naumov<sup>38</sup> reported 11.6% monomer and 88.3% dimer of  $\alpha$ -*trans*-cinnamic acid after 30 minutes photodimerization.

Viscosity and the  $T_g$  are the two parameters that can be used to assess the flexibility of the monomers. A precursory strong correlation exists among the base monomer's concentration,  $T_g$ , and DC in *bis*-GMA/TEGDMA composite systems.<sup>36</sup> The  $T_g$  of new polymeric restorative ought to be considered important to determine the clinical serviceability of the dental restoration.<sup>39</sup> Nevertheless,  $T_g$  is influenced by the cross-link density.<sup>40,41</sup> The difference in  $T_g$  between the groups is due to hindered allyl co-/homopolymerization of BD monomers and increased primary cyclization of TEGDMA in the C0, which results in microgelation and heterogeneous polymer network where the cross-linked regions that are loose and compact coexist. Cyclization leads to high local MPC% because it does not reduce the chain mobility in the matrix so much as cross-linking. Apparently, cyclization reduces the crosslinking density because cycles do not significantly contribute to the matrix network. As a result of cyclization, a polymerized composite resin would exhibit reduced  $T_g$ , mechanical strength, and solvent resistance.<sup>42,43</sup> The cyclization phenomenon of the TEGDMA was offset by its substitution and total replacement with PD-CMA in the E10 and

E20 groups, respectively. Since the trial groups exhibited higher  $T_g$  than the C0 group, it can be inferred that the PD-CMA imparted a homogeneous resin matrix resulting in highly cross-linked P (BD-Co-CMA) and P (B-Co-CMA) copolymers. Therefore, from the above context, the null hypothesis was rejected.

PD-CMA was substituted in the BD resin matrix at 10 wt. % and 20 wt. % concentrations in this current research. Beyond 20 wt. %, PD-CMA's capability to copolymerize with BD resin comonomers and its effect on MPC% and  $T_g$  has not been experimented with yet. Since the research is the first of its kind with CMA comonomer in a dental composite resin, prudent interpretation of the obtained results is mandatory. Prospective sequential studies should be attempted by increasing the CMA's concentration concerning the mechanical properties and biocompatibility.

## CONCLUSION

Within the research constraints, it was concluded that the incorporation of PD-CMA in the composite resin successfully copolymerized with the base matrix comonomers to form the novel P (BD-Co-CMA) and P (B-Co-CMA) copolymers. The P (B-Co-CMA) copolymer exhibited higher MPC% and  $T_g$  than the composite resin without PD-CMA.

## REFERENCES

- Mitra SB, Sakaguchi RL. Restorative materials - composites and polymers. In: Sakaguchi RL, Powers JM, (Eds). Craig's restorative dental materials. 13th edition. St. Louis: Mosby, 2013. pp. 161–198.
- Vasudeva G. Monomer systems for dental composites and their future. J Calif Dent Assoc 2009;37(6):389–398. PMID: 19831015.
- Santulli C. Nanostructured composites for dental fillings. In: Swain SK, Jawaid M, (Eds). Nanostructured polymer composites for biomedical applications. Amsterdam: Elsevier 2019. pp. 277–294. DOI: 10.1016/B978-0-12-816771-7.00014-4.
- Peutzfeldt A. Resin composites in dentistry: The monomer systems. Eur J Oral Sci 1997;105(2):97–116. DOI: 10.1111/j.1600-0722.1997.tb00188.x.
- Alshali RZ, Silikas N, Satterthwaite JD. Degree of conversion of bulk-fill compared to propriety resin-composites at two time intervals. Dent Mater 2013;29(9):e213–e217. DOI: 10.1016/j.dental.2013.05.011.
- Randolph LD, Palin WM, Bebelman S, et al. Ultra-fast light-curing resin composite with increased conversion and reduced monomer elution. Dent Mater 2014;30(5):594–604. DOI: 10.1016/j.dental.2014.02.023.



7. Par M, Gamulin O, Marovic D, et al. Raman spectroscopic assessment of degree of conversion of bulk-fill resin composites—changes at 24 hours post cure. *Oper Dent* 2015;40(3):E92–E101. DOI: 10.2341/14-091-L.
8. Sideridou ID, Tserki V, Papanastasiou G. Effect of chemical structure on degree of conversion in light-cured dimethacrylate-based dental resins. *Biomaterials* 2002;23(8):1819–1829. DOI: 10.1016/s0142-9612(01)00308-8.
9. Gajewski VE, Pfeifer CS, Frões-Salgado NR, et al. Monomers used in resin composites: Degree of conversion, mechanical properties and water sorption/solubility. *Braz Dent J* 2012;23(5):508–514. DOI: 10.1590/s0103-64402012000500007.
10. Stansbury JW. Dimethacrylate network formation and polymer property evolution as determined by the selection of monomers and curing conditions. *Dent Mater* 2012;28(1):13–22. DOI: 10.1016/j.dental.2011.09.005.
11. Leprince JG, Palin WM, Hadis MA, et al. Progress in dimethacrylate-based dental composite technology and curing efficiency. *Dent Mater* 2013;29(2):139–156. DOI: 10.1016/j.dental.2012.11.005.
12. Moldovan M, Balazsi R, Soanca A, et al. Evaluation of the degree of conversion, residual monomers and mechanical properties of some light-cured dental resin composites. *Materials (Basel)* 2019;12(13):2109. DOI: 10.3390/ma12132109.
13. Krzeminski M, Molinari M, Troyon M, et al. Calorimetric characterization of the heterogeneities produced by the radiation-induced cross-linking polymerization of aromatic diacrylates. *Macromolecules* 2010;43(8):3757–3763. DOI: 10.1021/ma902817g.
14. Chung CM, Kim MS, Kim JG, et al. Synthesis and photopolymerization of trifunctional methacrylates and their application as dental monomers. *J Biomed Mater Res* 2002;62(4):622–627. DOI: 10.1002/jbm.10359.
15. Ferracane JL. Hygroscopic and hydrolytic effects in dental polymer networks. *Dent Mater* 2006;22(3):211–222. DOI: 10.1016/j.dental.2005.05.005.
16. Asmussen E, Peutzfeldt A. Influence of pulse-delay curing on softening of polymer structures. *J Dent Res* 2001;80(6):1570–1573. DOI: 10.1177/00220345010800061801.
17. Ajay R, Suma K, Ali SA. Monomer modifications of denture base acrylic resin: A systematic review and meta-analysis. *J Pharm Bioall Sci* 2019;11(Suppl 2):S112–S125. DOI: 10.4103/JPBS.JPBS\_34\_19.
18. Sivakumar JS, Ajay R, Sudhakar V, et al. Chemical characterization and physical properties of dental restorative composite resin with a novel multifunctional cross-linking comonomer. *J Contemp Dent Pract* 2021;22(6):630–636. PMID: 34393119.
19. Viljanen EK, Skrifvars M, Vallittu PK. Dendritic copolymers and particulate filler composites for dental applications: Degree of conversion and thermal properties. *Dent Mater* 2007;23(11):1420–1427. DOI: 10.1016/j.dental.2006.11.028.
20. Zhang Y, Zhang D, Qin C, et al. Physical and mechanical properties of dental nanocomposites composed of aliphatic epoxy resin and epoxidized aromatic hyperbranched polymers. *Polym Compos* 2008;30(2):176–181. DOI: 10.1002/pc.20549.
21. Minsk LM, Smith JG, van Deusen WP, et al. Photosensitive polymers. I. Cinnamate esters of poly(vinylalcohol) and cellulose. *J Appl Polym Sci* 1959;2(6):302–307. DOI: 10.1002/app.1959.070020607.
22. Oya N, Sukarsaatmadja P, Ishida K, et al. Photoinduced mendable network polymer from poly(butylene adipate) end-functionalized with cinnamoyl groups. *Polym J* 2012;44:724–729. DOI: 10.1038/pj.2012.18.
23. Tunc D, le Coz C, Alexandre M, et al. Reversible cross-linking of aliphatic polyamides bearing thermos- and photoresponsive cinnamoyl moieties. *Macromolecules* 2014;47(23):8247–8254. DOI: 10.1021/ma502083p.
24. Imada M, Takenaka Y, Hatanaka H, et al. Unique acrylic resins with aromatic side chains by homopolymerization of cinnamic monomers. *Commun Chem* 2019;2:109. DOI: 10.1038/s42004-019-0215-3.
25. Nomoto R, Asada M, McCabe JF, et al. Light exposure required for optimum conversion of light activated resin systems. *Dent Mater* 2006;22(12):1135–1142. DOI: 10.1016/j.dental.2005.10.011.
26. Ajay R, Suma K, Sasikala R, et al. Chemical structure and physical properties of heat-cured poly (methyl methacrylate) resin processed with cycloaliphatic comonomer: An *in vitro* study. *J Contemp Dent Pract* 2020;21(3):285–290. DOI: 10.4103/jpbs.jpbs\_20\_20.
27. Asmussen E, Peutzfeldt A. Influence of UEDMA BisGMA and TEGDMA on selected mechanical properties of experimental resin composites. *Dent Mater* 1998;14(1):51–56. DOI: 10.1016/s0109-5641(98)00009-8.
28. Lemon MT, Jones MS, Stansbury JW. Hydrogen bonding interactions in methacrylate monomers and polymers. *J Biomed Mater Res A* 2007;83(3):734–746. DOI: 10.1002/jbm.a.31448.
29. Sideridou ID, Karabela MM, Bikiaris DN. Aging studies of light cured dimethacrylate-based dental resins and a resin composite in water or ethanol/water. *Dent Mater* 2007;23(9):1142–1149. DOI: 10.1016/j.dental.2006.06.049.
30. Gonçalves F, Pfeifer CC, Stansbury JW, et al. Influence of matrix composition on polymerization stress development of experimental composites. *Dent Mater* 2010;26(7):697–703. DOI: 10.1016/j.dental.2010.03.014.
31. Janda R, Roulet JF, Latta M, et al. Water sorption and solubility of contemporary resin-based filling materials. *J Biomed Mater Res B Appl Biomater* 2007;82(2):545–551. DOI: 10.1002/jbm.b.30760.
32. Sideridou ID, Karabela MM, Vouvoudi ECh. Dynamic thermomechanical properties and sorption characteristics of two commercial light cured dental resin composites. *Dent Mater* 2008;24(6):737–743. DOI: 10.1016/j.dental.2007.08.004.
33. Lovell LG, Newman SM, Bowman CN. The effects of light intensity, temperature, and comonomer composition on the polymerization behavior of dimethacrylate dental resins. *J Dent Res* 1999;78(8):1469–1476. DOI: 10.1177/00220345990780081301.
34. Wollff EM. The effect of cross-linking agents on acrylic resins. *Aust Dent J* 1962;7(6):439–444. DOI: 10.1111/j.1834-7819.1962.tb02619.x.
35. Atkinson SD, Almond MJ, Hollins P, et al. The photodimerisation of the alpha- and beta-forms of trans-cinnamic acid: A study of single crystals by vibrational microspectroscopy. *Spectrochim Acta A Mol Biomol Spectrosc* 2003;59(3):629–635. DOI: 10.1016/s1386-1425(02)00208-1.
36. Chroszcz M, Barszczewska-Rybark I. Synthesis of novel urethane-dimethacrylate monomer containing two quaternary ammonium groups for applications in dentistry. *Proceedings* 2020;67(1):3. DOI: 10.3390/ASEC2020-07548.
37. Al-Odayni AB, Alfortawi R, Khan R, et al. Synthesis of chemically modified BisGMA analog with low viscosity and potential physical and biological properties for dental resin composite. *Dent Mater* 2019;35(11):1532–1544. DOI: 10.1016/j.dental.2019.07.013.
38. Panda T, Naumov P. Time-dependent photodimerization of  $\alpha$ -trans-cinnamic acid studied by photocalorimetry and NMR spectroscopy. *Cryst Growth Des* 2018;18(5):2744–2749. DOI: 10.1021/acs.cgd.7b01409.
39. Wong K, Boyde A, Howell PGT. A model of temperature transients in dental implants. *Biomaterials* 2001;22(20):2795–2797. DOI: 10.1016/s0142-9612(01)00023-0.
40. Greenberg AR, Kusy RP. Influence of crosslinking on the glass transition of poly(acrylic acid). *J Appl Polym Sci* 1980;25(8):1785–1788. DOI: 10.1002/app.1980.070250825.
41. Luo Z, Yang Z, Fei Z, et al. Effect of crosslinking rate on the glass transition temperature of polyimide cross-linked silica aerogels. *J Polym Res* 2020;27(9):255. DOI: 10.1007/s10965-020-02082-9.
42. Boots HMJ, Pandey RB. Qualitative percolation study of free-radical cross-linking polymerization. *Polym Bull* 1984;11:415–420. DOI: 10.1007/BF00265480.
43. Anseth KS, Bowman CN. Kinetic gelation model predictions of crosslinked polymer network microstructure. *Chem Eng Sci* 1994;49(14):2207–2217. DOI: 10.1016/0009-2509(94)E0055-U.